Journal of Advanced Research 18 (2019) 71–79

Contents lists available at ScienceDirect

Journal of Advanced Research

journal homepage: www.elsevier.com/locate/jare

Original article

Trehalase localization in the cerebral cortex, hippocampus and cerebellum of mouse brains

L. Halbe, A. Rami *

Institut für Zelluläre und Molekulare Anatomie (Anatomie III), Klinikum der Johann Wolfgang von Goethe-Universität, Theodor-Stern-Kai 7, 60590 Frankfurt/Main, Germany

HIGHLIGHTS

- Morphological localization of trehalase *in vivo* in the mouse brain.
- Exclusive expression of trehalase in neurons.
- Astrocytes do not express trehalase.
- A strong trehalase-immunoreactivity of trehalase was found in the perikarya and dendrites of neurons.
- Trehalase levels in neurons should have a physiological significance.

GRAPHICAL ABSTRACT

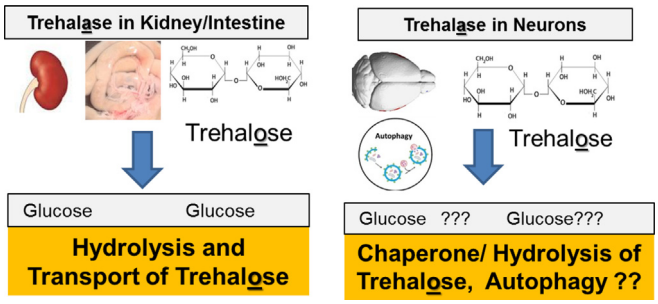

ARTICLE INFO

Article history:
Received 22 November 2018
Revised 18 January 2019
Accepted 21 January 2019
Available online 25 January 2019

Keywords:
Trehalase
Trehalose
Hippocampus
Cerebral cortex
Cerebellum
Mice

ABSTRACT

The non-reducing disaccharide trehalose is biosynthesized in several species but not in vertebrates. However, trehalase, the enzyme required for its cleavage, has been observed in different mammalian organs. Even in humans, trehalase was detected in the gastrointestinal tract and the kidney. Trehalase is an intrinsic glycoprotein of the small intestine and kidney that transports trehalose and hydrolyses it to two glucose molecules. To our knowledge, no information is available about the *in vivo* distribution and localization of trehalase in the mammalian brain. Here, we report the occurrence and distribution of trehalase *in vivo* in the mouse brain using Western blotting and immunohistochemical techniques. Using an antibody against trehalase, we demonstrated that the enzyme showed a band with a molecular mass of approx. 70 kDa in the hippocampus, cerebral cortex, cerebellum and olfactory bulbs. Strong trehalase immunoreactivity was found in the perikarya and dendrites of neurons located in the hippocampus, cerebral cortex, Purkinje cells and mitral cells. Interestingly, Purkinje cells of the cerebellum showed higher immunoreactivity than neurons in the hippocampus and cerebral cortex. The distribution of trehalase appeared to be mainly related to neurons and was not detected in astrocytes. Independent of the presence of trehalose in neurons, the trehalase levels in neurons should have physiological significance. Investigating whether the interactions between trehalose and trehalase act on brain energy metabolism or have other not-yet-identified effects would also be interesting.

Introduction

Trehalose is a non-reducing and conserved disaccharide in prokaryotes, eukaryotes and invertebrates, but its biosynthesis does not occur in vertebrates and mammals [1]. This sugar was first described in the haemolymph [2] and muscles of insects as a source of energy during flight [3]. Trehalose exhibits specific physical properties, such as high chemical stability and strong resistance to cleavage by glucosidases. Recent data demonstrate that trehalose can act as a molecular chaperone conferring cell resistance against oxidative stress, heat and dehydration. Furthermore, trehalose has been shown to be capable of reducing the amyloid

Peer review under responsibility of Cairo University.
* Corresponding author.
E-mail address: Rami@em.uni-frankfurt.de (A. Rami).

https://doi.org/10.1016/j.jare.2019.01.009
2090-1232/

formation caused by insulin *in vitro* [4] and attenuating beta amyloid deposition associated with AD pathology [5,6]. Trehalose can also ameliorate pathological features of Huntington's disease in mouse models [6–8], delay the progression of the amyotrophic lateral sclerosis (ALS) [9] and reduce retinal degeneration upon lysosomal hydrolase deficiency [9]. Trehalose reduced accumulation of misfolded proteins, such as, polyglutamine aggregates, mutant SOD1 [10,11], synuclein [12–14], prion protein [15,16], TDP-43 [17]. In addition trehalose also acts as an anti-oxidant and anti-inflammatory molecule [18–21]. Lotfi et al. [22] elegantly showed that trehalose induces autophagy in the retina and increases the removal of autophagic vacuoles in a murine model of brain mucopolysaccharidosis IIIB. Mounting experimental evidence suggests that trehalose modulates pathophysiological events through multiple processes and may prevent neurodegenerative diseases by stabilizing proteins and promoting autophagy [23]. Recently Mardones et al. [24] have shown that trehalose inhibits cellular import of glucose through SLC2A (GLUT) transporters, generating a starvation-like state that stimulates autophagy. In addition to the autophagy-induction, the effects of trehalose might be exerted through microbiota-gut-brain signaling, mostly that gut microbiota play a central role on many physiological systems, including the CNS [25]. However, further studies would be needed to elucidate the mechanism underlying how trehalose reaches the cells and activates autophagy in the brain. Almost, trehalose has been considered generally regarded as safe by the FDA and is currently being tested in several clinical trials as an autophagy modulator. All of these properties make this disaccharide very attractive as a potential therapeutic strategy for many neurodegenerative diseases.

Intriguingly, vertebrates do not synthetize trehalose, even though they express significant amounts of trehalase [2]. Previous data from Ruf et al. [26] showed that trehalases are relatively similar in mammals and yeast and can be induced under oxidative stress and starvation [26]. In addition, deletion of yeast trehalase increases the vulnerability of cells to heat shock compared with that of wild-type cells [27].

As already mentioned, trehalase constitutes an intrinsic glycoprotein of the small intestine and renal membranes in animals [28–31] and is involved in sugar transport across the brush-border membranes in the kidney and hydrolysis of ingested trehalose in the intestine [31]. In fact, people exhibiting intestinal trehalase deficiency suffer from diarrhoea after consuming products containing trehalose, such as mushrooms [32]. In addition, the presence of trehalase in urine was recently demonstrated to be a specific index of renal tubular deficiency [33]. Furthermore, the activity of trehalase was elevated in patients with diabetes mellitus and rheumatoid arthritis [34–37] and [41–43].

To our knowledge, no information is available about the *in vivo* distribution and localization of trehalase in the brain. Here, we report the *in vivo* occurrence and distribution of trehalase in the mouse brain using Western blotting and immunohistochemical techniques.

Material and methods

Animals

All animal experiments were performed as approved by the Policy on the Use of Animals in Neuroscience Research, the Policy on Ethics of the Society for Neuroscience, the Federal Guidelines and the European Communities Council Directive (89/609/EEC), and the local veterinary administration (approval file number: FU/1045). Male C57BL/6 mice aged 9–12 weeks were purchased from Janvier Labs (France). Mice were maintained under a standard 12:12 light/dark cycle with 12 h of light and 12 h of darkness. Animals were kept at constant room temperature with food and water available ad libitum. Tissue sampling was carried out when animals were sacrificed under deep anaesthesia.

Immunofluorescence

Mice (n = 12) were anaesthetized with an overdose of pentobarbital (100 mg/kg i.p.) and were perfused transcardially with saline followed by paraformaldehyde solution (4% in 0.02 M phosphate-buffered saline (PBS)). Brains were cut into 12 μm thick sections in the coronal plane on a cryostat. For immunofluorescence, sections were treated for 1 h with PBS containing 5% normal goat serum (NGS; Sigma, Germany). Thereafter, sections were incubated with primary antibodies at 4 °C for 24 h. Mouse monoclonal antibodies raised against trehalase (Santa Cruz/sc-390034, Heidelberg, Germany), rabbit monoclonal anti-NeuN (Cell Signaling, Germany), and mouse monoclonal anti-GFAP (Sigma, Germany) were used. After several washes in 0.1 M PBS, sections were incubated with Alexa Fluor 488- or 568-conjugated anti-mouse IgG (1:200, 2 h, in 0.1 M PBS; Molecular Probes, Eugene, Germany). After rinsing with PBS, the sections were mounted in Dako fluorescent mounting medium containing DAPI (Dako, Hamburg, Germany). For the assessment of non-specific immunostaining, alternating sections from each experimental group were preincubated for 1 h with the corresponding blocking peptide (Sigma, Heidelberg, Germany). To validate the specificity of the antibody raised against trehalase, histological sections from the intestine and kidney were used as positive controls (see Fig. 1). Small blocks of kidney and intestine were removed from paraformaldehyde-perfused mice (n = 3) and sectioned at a thickness of 12 μm. The sections were washed thoroughly with PBS and incubated with anti-trehalase IgG (1:250).

Digital illustrations

Fluorescent images were acquired using an Axio-Cam digital camera mounted on a Zeiss microscope (Carl Zeiss, Jena, Germany). Single fluorescent images of the same section were digitally superimposed. For semiquantitative densitometric analyses of the immunoreactions, images were digitized using NIH ImageJ software (Image Processing and Analysis in Java, developer Wayne Rasband, USA). Regions of the hippocampal formation, cortex, cerebellum and olfactory bulbs were selected individually, and the relative optical density (rel. O.D.) to background staining was measured within selected areas. Subsequently, the values were averaged for each animal (7 to 10 sections per animal).

Preparation of tissue and Western blotting

Mice (n = 6) were anaesthetized with an overdose of pentobarbital (100 mg/kg i.p.). Small blocks of the cerebral cortex, cerebellum, hippocampus, olfactory bulbs, kidney and intestine were processed (blocks of intestine and kidney served as positive controls). Aliquots were stored at −80 °C, and 30 μg of total protein was used per lane. Samples were resuspended to contain 30 μg of total protein in loading buffer and heated for 5 min at 95 °C. Samples were separated on a 4–12% Bis-Tris gel with MES SDS running buffer using an electrophoresis system (Invitrogen). Gels were run at 200 V for 55 min and subsequently electroblotted to a PVDF membrane with iBlot. Blots were blocked with Rotiblock (Carl Roth, Germany) for 1 h at room temperature to reduce non-specific binding of antibodies. Anti-mouse monoclonal antibodies raised against trehalase (Santa Cruz/sc-390034, Heidelberg, Germany) were used at a 1:500 dilution. β-Actin (Sigma-Aldrich, USA) (dilution 1:40,000) was used as a control protein, and

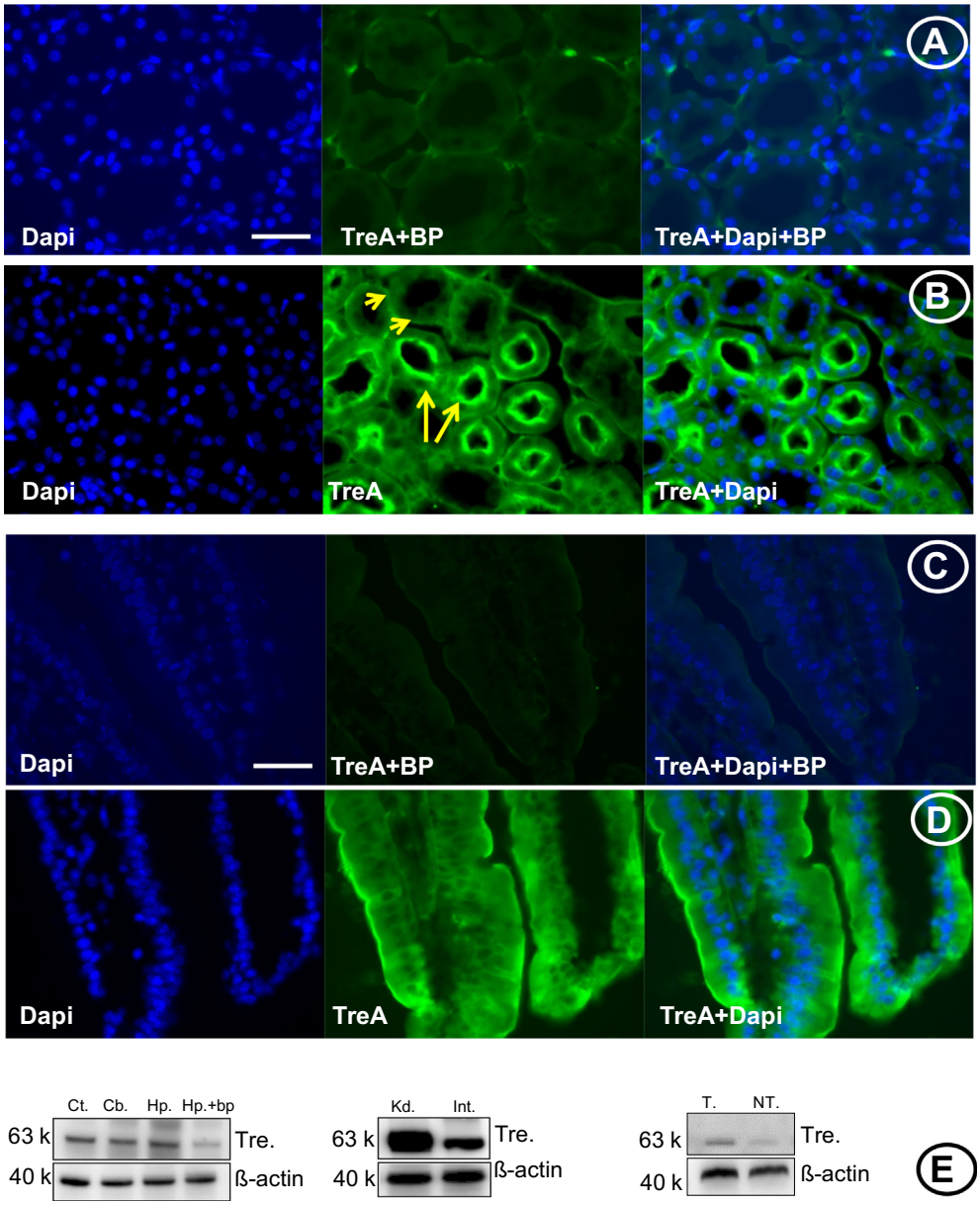

Fig. 1. Sections of kidney (B) and intestine (D) treated with anti-trehalase and DAPI. The sections of kidney treated with anti-trehalase showed clearly defined fluorescence at the brush border of the proximal tubules (arrows) with no specific fluorescence in the distal tubules (arrowheads). A and C show sections of kidney and intestine, respectively, assessed by the adsorption of the primary antibody with the corresponding blocking peptide as negative controls. The immunoreactivity was abolished upon preincubation of trehalase-antibody with the corresponding antigenic peptide. E shows a positive band at 63 kDa in the cerebral cortex, intestine and kidney (Abbr.: TreA; trehalase, (-)TreA, without trehalase, Ctx; cerebral cortex, Int.; intestine, Kid.; kidney). Scale bar: 80 μm.

anti-rabbit IgG (Santa Cruz, USA) (1:30,000) and anti-mouse IgG (P0447 Dako, Germany) (1:30,000) were used as secondary antibodies. To validate the specificity of the antibody raised against trehalase, mouse trehalase transfected 293 T whole cell lysate (Sant cruz, Heidelberg, Germany, sc-124274) were used as positive controls and mouse non-transfected cell lysates (Santa cruz, Heidelberg, Germany, sc-117752) were used as negative controls. Signals were detected using Immobilon Western Chemoluminescent HRP Substrate (Millipore, Billerica, USA), digitized using a Chemi-Doc XRS System (Bio-Rad, München, Germany) and analysed using a luminescence system (Quantity One, ChemiDoc XRS, Bio-Rad, Hercules, CA, USA). probes from the intestine and kidney were used as positive controls (see Fig. 1). The optical intensity of all target signals on any given Western blot (n = 3 to 6) was always normalized to the optical intensity of the actin signal on the same blot. The normalized signal intensities were then expressed as relative signal intensities (O.D.). In separate control experiments with the trehalase antibody, membranes were preincubated for 1 h with the corresponding blocking peptide (Sigma, Heidelberg, Germany). Protein expression levels were quantified using gel analysis software ImageJ (v1.44p for Windows, National Institute of Health, Bethesda, USA).

Statistical analysis

Statistical evaluation was performed with GraphPad Prism 3.0 (GraphPad, San Diego, CA, USA). Data are reported as the means ± SEM of n experiments (n = 6 or more). Means were compared with One-way analysis of variance (ANOVA) with Bonferroni's multiple comparison test, to estimate differences between examined groups. Significant differences between means at each time point

were assessed by unpaired Student's *t*-test ($^{*}P < 0.05$, $^{**}P < 0.01$ and $^{***}P < 0.001$ were considered statistically significant).

Results

This paper addresses the distribution of trehalase in the normal adult mouse brain. To validate the specificity of the trehalase antibody used, histological sections from the intestine and kidney were used as positive controls. As shown in Fig. 1, the sections treated with anti-trehalase showed clearly defined fluorescence in enterocytes (Fig. 1C-D) and at the brush border of proximal tubules (with no specific fluorescence in distal tubules) (Fig. 1A-B). When we probed homogenates of cerebral cortex, intestine and kidney with the primary antibody, we detected a protein band at approx. 70 kDa (Fig. 1E). The signals were abolished upon preincubation of trehalase-antibody with corresponding antigenic peptide.

As shown in Figs. 2–4, the sections of mouse brains treated with anti-trehalase showed clearly defined fluorescence in the hippocampus, cerebral cortex and cerebellum. Moreover, these results

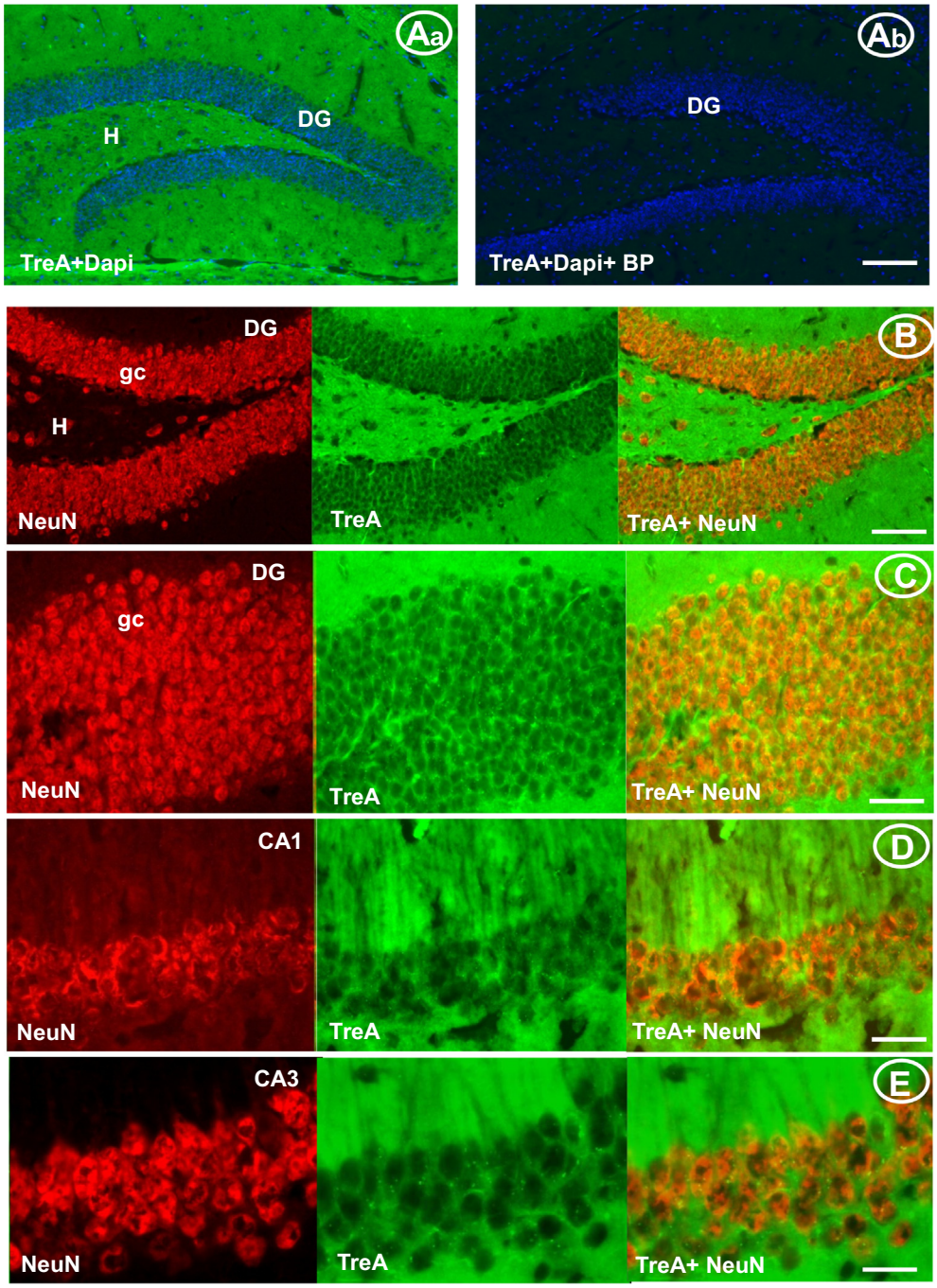

Fig. 2. Representative immunohistochemical staining for trehalase. (Aa) Brain section treated with anti-trehalase antibody (green) and Dapi (blue). (Ab) The immunoreactivity (green) was abolished upon preincubation of trehalase-antibody with the corresponding antigenic peptide. Trehalase immunoreactivity was detected in the dentate gyrus (B-C) and in the Ammoń s horn of the hippocampal formation (D-E). Granule cells of the dentate gyrus and pyramidal cells of the CA1- and CA3-subfields were trehalase-immunoreactive (green). Trehalase immunoreactivity was localized in the cytosol as well as in dendrites. Neurons have been characterized with NeuN (red). (Abbr.: DG; Dentate gyrus, gc; granule cells, H; hilus, ml; molecular layer; NeuN; neuronal marker, TreA; trehalase, BP; blocking peptide). Scale bars: 100 μm in A; 80 μm in B; 50 μM in C-D-E.

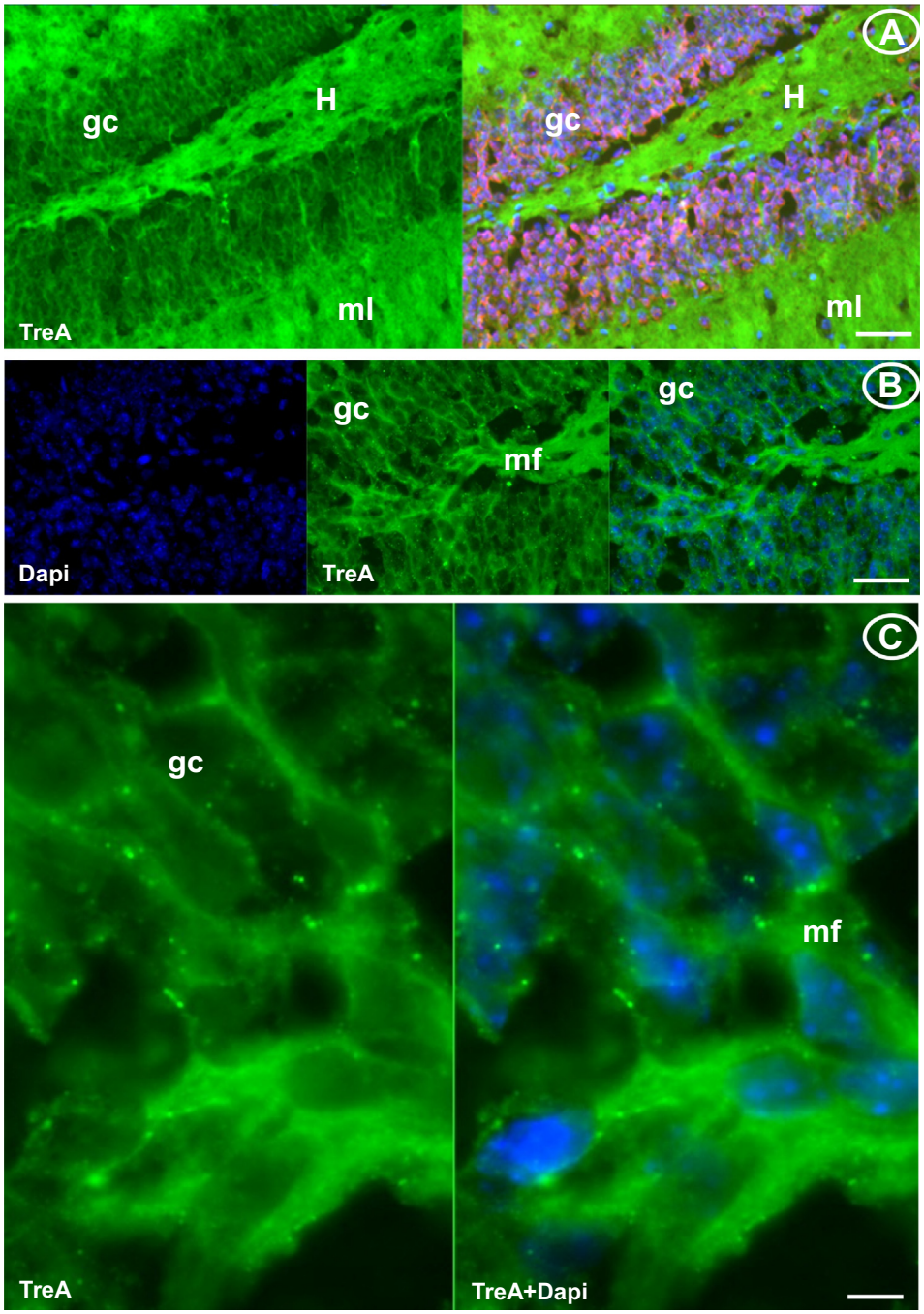

Fig. 3. Details of trehalase immunoreactivity in the dentate gyrus (triple staining with DAPI (blue), NeuN (red) and trehalase (treA- green) in A and double staining with DAPI (blue) and trehalase (green) in B and C). Trehalase immunoreactivity was seen in the granule cells, including the molecular layer (ml) and the hilus (H). B clearly shows the trehalase immunoreactivity in the perikarya as well as in the axons of granule cells, the so-called mossy fibres (mf). Scale bars: 100 μm in A, 70 μm in B and 50 μm in C.

coincided with the biochemical results of Western blotting, indicating the localization of trehalase in the hippocampus, cerebral cortex and cerebellum (Fig. 5E). No signals were detected in Western blots with trehalase antibody, when they were pre-incubated with the corresponding antigenic peptides (Fig. 5E).

In the hippocampal formation, trehalase antibody showed moderate immunoreactivity (IR) in all parts of the granule cells in the dentate gyrus (soma, dendrites, axons). However, axons of the granule cells, the so-called mossy fibres, were detectable only in the hilus (Fig. 3B-C). Moreover, the hilus of the dentate gyrus showed stronger trehalase-immunoreactivity than the granular layer (Figs. 2B & 3A-B). The immunostaining in the molecular layer of the dentate gyrus was homogeneous and diffuse. Pyramidal neurons located in the CA1, CA2, CA3 and CA4 subfields exhibited clear trehalase-IR in their soma and dendrites, but without any discrete differences between the different hippocampal subfields (Fig. 2D-E).

Fig. 3A shows representative views of the cerebral cortex. Immunostaining with the trehalase antibody in the cerebral cortex showed homogeneous and strong labelling of all cortical layers. In these layers, most pyramidal cells, their dendrites and the surrounding neuropil were trehalase-immunopositive. Positive axons

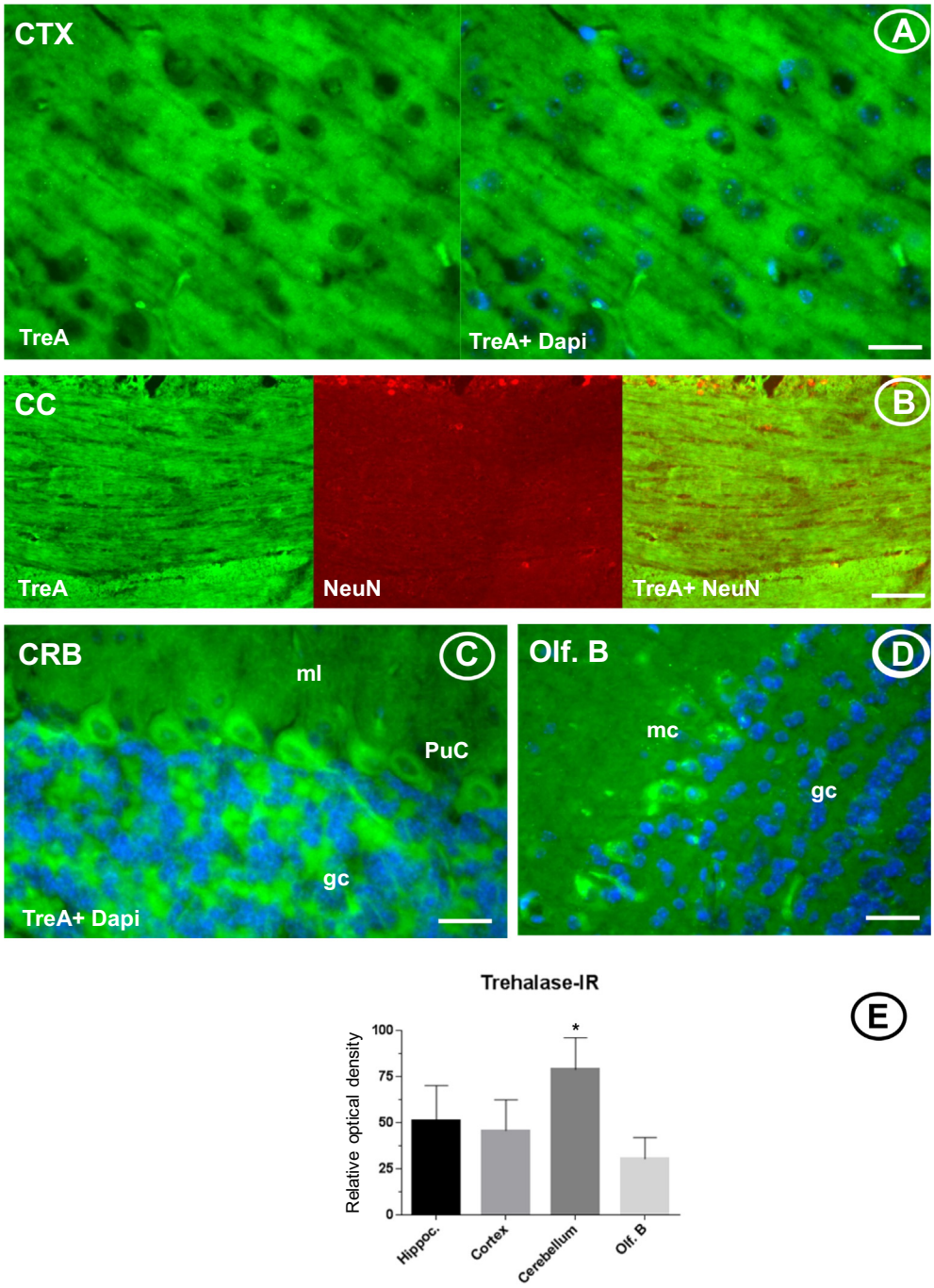

Fig. 4. (A) In the cerebral cortex (CTX), immunostaining showed fairly homogeneous and strong labelling of all cortical layers. In these layers, most pyramidal cells and the neuropil were stained. Trehalase-positive dendrites came in close contiguity to each other or to trehalase-positive perikarya. Positive axons were difficult to discern because of their thinness, but they leave left the cortical mantle, e.g., through the corpus callosum (B). (C) In the cerebellum (CRB), trehalase immunoreactivity was clearly observed in the Purkinje neurons (PuC), molecular layer (ml) and granule cells (gc). (D) shows a slight trehalase immunoreactivity in the mitral cells of the olfactory bulbs. (E) Densitometric analysis of trehalase immunofluorescence showed differences between the hippocampus, cerebral cortex and cerebellum. The highest trehalase immunoreactivity was found in the cerebellum and especially in the Purkinje cells. Values (n = 6/group with 7–10 sections/animal) are expressed as the mean ± SEM. ($^{*}P < 0.05$ different from cortex and hippocampus). Scale bars: 100 μm in A-C-D and 70 μm in B.

were difficult to detect within the cerebral cortex, but they could be clearly observed in the corpus callosum (Fig. 4B).

In the cerebellum (Fig. 4C), the molecular layer was immunoreactive, as were the granule and Purkinje neurons. Interestingly, we observed higher trehalase-IR in the cerebellum compared to other brain regions (Fig. 4E). In particular, Purkinje cells exhibited the highest trehalase-IR among all examined areas. In the granular layer, immunoreactivity was observed in most granule cells. Immunoreactivity to trehalase was also observed in axon terminals distributed throughout the cerebellar cortex (Fig. 4B). In the olfactory bulbs (OB), trehalase immunoreactivity was seen in the mitral cells (Fig. 4D).

Since immunoreactivity was mainly detected in neurons, establishing whether trehalase exhibits immunoreactivity in astrocytes was of interest. However, no evidence was found for the co-existence of trehalase and GFAP in astrocytes in any of the exam-

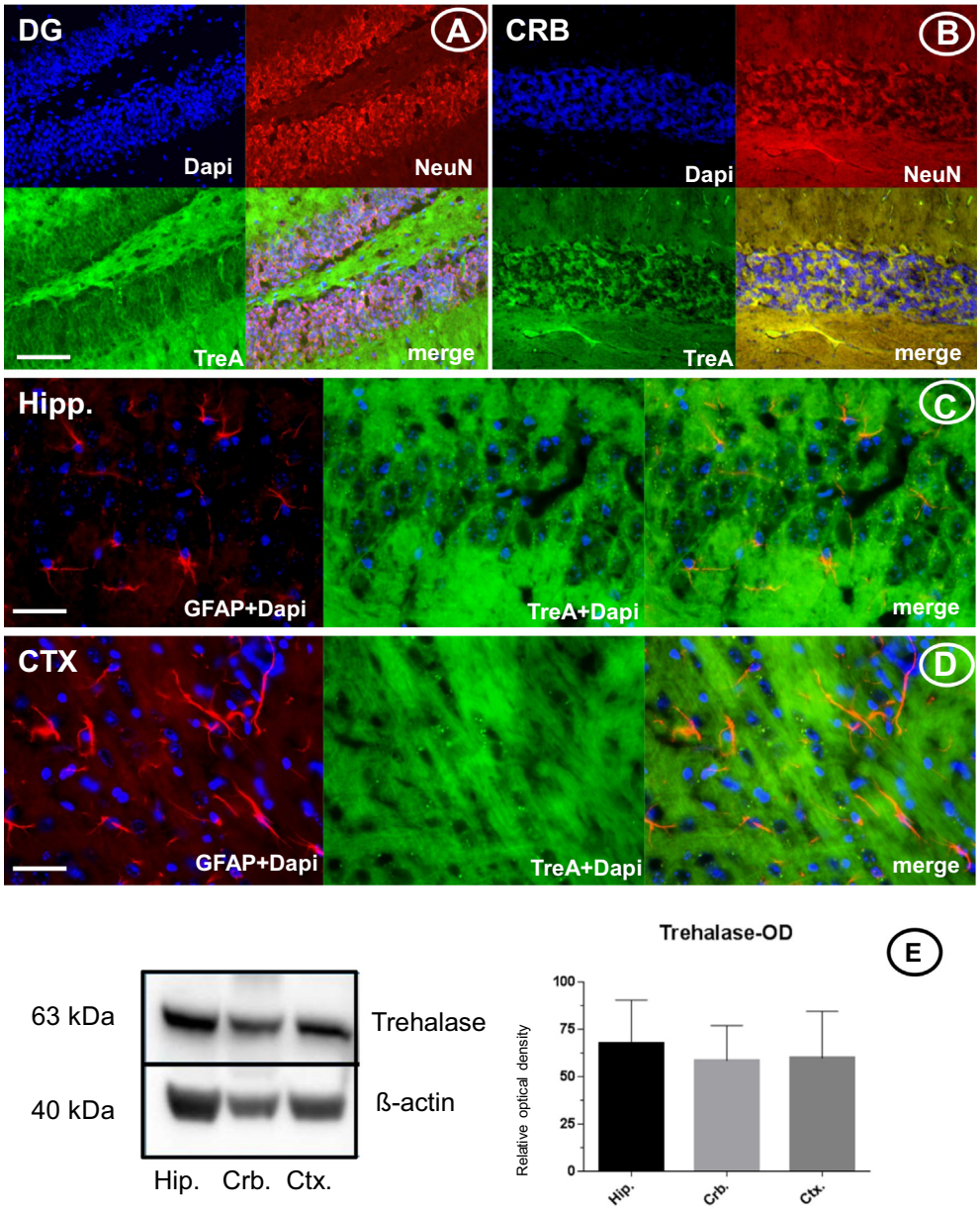

Fig. 5. A & B show double immunostaining for trehalase (green) and NeuN (red) in the dentate gyrus (A) and cerebellum (B). C and D show double immunostaining for trehalase (green) and GFAP (red) in the hippocampus (C) and cerebral cortex (D). No evidence for the co-existence of trehalase and GFAP in any examined areas (C and D). However, trehalase-IR was strictly correlated with NeuN-immunoreactive cells in all examined areas, which confirms neuronal localization. (E) Immunoblotting of trehalase levels in the hippocampus (hip.), cerebral cortex (Ctx.) and cerebellum (Crb.). Using an antibody against trehalase, we demonstrated that the enzyme showed a band with a molecular mass of approx. 63 kDa. (Abbr.: DG; dentate gyrus, Hip; hippocampus, TreA; trehalase, CTX; cerebral cortex, CRB; cerebellum). Scale bars: 100 μm in A-B and 70 μm in C-D.

ined areas (Fig. 5C-D). Interestingly, trehalase-IR was strictly correlated with the neuronal marker NeuN in all examined areas, which confirmed the strict neuronal localization (Fig. 5A-B).

Discussion

In mammals, although trehalose biosynthetic genes are missing, two trehalose-hydrolysing enzymes are detectable. These enzymes act as intrinsic glycoproteins of the intestine and renal brush-border membranes. Until now, intestinal trehalase was known to be the sole hydrolase that is capable of cleaving trehalose, and in this context, deficiency in its catalytic activity leads to severe digestive disorders in mammals. Individuals with trehalase deficiency suffer abdominal pain after consuming foods containing trehalose [32]. The emerging symptoms include, for instance, bloating, abdominal pain and diarrhoea. These symptoms can be abolished upon treatment with the probiotic *Saccharomyces boulardii,* which can deliver trehalase in to the gastrointestinal tract [38-40].

The fact that trehalase is expressed in the small intestine of several mammalian species, although these species do not synthesize trehalose, is at the same time fascinating and not surprising. This finding is not surprising because mammals, including humans, can use trehalose as nutrition [35]. Lotfi et al. [22] recently reported a positive correlation between trehalose in food consumption and brain bioavailability of trehalose in mice. In addition, mammals express trehalase during gestation, and the highest concentrations are reached after parturition [39], suggesting that trehalase might be an important enzyme in the early stages of life [39].

Nevertheless, no information was available about the expression and distribution of trehalase in the nervous system. Here, we report on the expression of trehalase in the hippocampus, cerebral cortex, cerebellum and olfactory bulbs of mice. Trehalase immunoreactivity was found in the perikarya, dendrites and axons of neurons, with higher expression in Purkinje neurons compared to that in the other brain areas. Moreover, the distribution of trehalase appears to be exclusively related to neurons; trehalase was not detected in astrocytes. The function of the enzyme in these locations is not known. On the basis of the fact that trehalase localizes in neurons but not in astrocytes, Martano et al. [44] suggest the existence of a novel neuro-glia metabolic pathway [44].

Recently, Mayer et al. [45] reported that trehalose transport in hepatocytes is carrier-mediated and that the Glut8 transporter is indispensable for trehalose-mediated autophagy [45]. Interestingly, trehalase and Glut8 exhibited the same cellular distribution and are both expressed in neurons and not in glial cells. Thus, the co-existence of trehalase and Glut8 in neurons should have, to some extent, functional importance.

Interestingly, Chen et al. [46] have shown that trehalase plays an important role in the maintenance of neuroepithelial stem cells in the Drosophila optic lobe. Loss of trehalase function causes neuroepithelial damage and a drastic reduction in precursor cell density [46]. The authors also showed that exogenous glucose was not able to compensate for the loss of trehalase. This finding indicates that trehalase may regulate neuroepithelial maintenance and differentiation independently of its hydrolase activity.

Martano et al. [44] were the first to detect trehalose in rodent hippocampus and showed that trehalose influences the morphology of neurons by increasing dendritic arborization during neuronal maturation [44]. These authors have suggested that neurons are the main consumers of trehalose, but the source of trehalose was unclear.

Interestingly, human trehalase increased the vulnerability of yeast to various stressors, such as heat shock, oxidative stress, and osmotic stress, resulting in cell death [47]. These results suggest that human trehalase is a stress-response protein in the kidney rather than being involved in the utilization of exogenous trehalose [47].

Conclusions

The function of trehalase in the nervous system is not known; however, mammalian trehalase may also have hydrolase-independent functions and perhaps play a role in the maintenance and differentiation of cells during brain development. Questions concerning the fate of trehalose in neurons expressing trehalase and the function of trehalase in neurons are important. Independent of the presence of trehalose in neurons, the trehalase levels in neurons should have physiological significance. Furthermore, investigating whether the interactions between trehalose and trehalase act on brain energy metabolism or have other not-yet-identified effects would also be interesting.

Conflict of interest

The authors have declared no conflict of interest.

Acknowledgements

We thank Alena Konoplew for expert technical support. We thank Professor J. Stehle for scientific support of our work. This work was supported partly by the Adolf-Messer-Stiftung (grant to A. Rami – "Molecular mechanisms of autophagy"). L. Halbe was supported partly by the AMS and the FPF (Frankfurter Promotionsförderung).

References

[1] Richards AB, Krakowka S, Dexter LB, Schmid H, Wolterbeek AP, Waalkens-Berendsen DH, et al. Trehalose: a review of properties, history of use and human tolerance, and results of multiple safety studies. Food Chem Toxicol 2002;40(7):871–98.
[2] Sacktor B. Biochemical adaptations for flight in the insect. Biochem Soc Symp 1976;41:111–31.
[3] Elbein AD, Pan YT, Pastuszak I, Caroll D. New insights on trehalose: a multifunctional molecule. Glycobiology 2003;13(4):17R–27R.
[4] Arora A, Ha C, Park CB. Inhibition of insulin amyloid formation by small stress molecules. FEBS Lett 2004;564(1–2):121–5.
[5] Du J, Liang Y, Xu F, Sun B, Wang Z. Trehalose rescues Alzheimer's disease phenotypes in APP/PS1 transgenic mice. J Pharm Pharmacol 2013;65(12):1753–6.
[6] Portbury SD, Hare DJ, Sgambelloni C, et al. Trehalose improves cognition in the transgenic Tg2576 mouse model of Alzheimer's disease. J Alzheimers Dis 2017;60:549–60.
[7] Tanaka M, Machida Y, Niu S, Ikeda T, Jana NR, Doi H, et al. Trehalose alleviates polyglutamine-mediated pathology in a mouse model of Huntington disease. Nat Med 2004;10(2):148–54.
[8] Sarkar S, Rubinsztein DC. Huntington's disease. Degradation of mutant huntingtin by autophagy. FEBS J 2008;275:4263–70.
[9] Castillo K, Nassif M, Valenzuela V, Rojas F, Matus S, Mercado G, et al. Trehalose delays the progression of amyotrophic lateral sclerosis by enhancing autophagy in motoneurons. Autophagy 2013;9(9):1308–20.
[10] Höller CJ, Taylor G, McEachin ZT, Deng Q, Watkins WJ, Hudson K, et al. Trehalose upregulates progranulin expression in human and mouse models of GRN haplosufficiency: a novel therapeutic lead to treat frontotemporal dementia. Mol Neurodegenerat 2016;11(1):46.
[11] Li Y, Guo Y, Wang X, Yu X, Duan W, Hong K, et al. Trehalose decreases mutant SOD1 expression and alleviates motor deficiency in early but not end-stage amyotrophic lateral sclerosis in a SOD1-G93A mouse model. Neuroscience 2015;298:12–25.
[12] Casarejos MJ, Solano RM, Gomez A, Perucho J, de Yebenes JG, Mena MA. The accumulation of neurotoxic proteins, induced by proteasome inhibition, is reverted by trehalose, an enhancer of autophagy, in human neuroblastoma cells. Neurochem Int 2011;58(4):512–20.
[13] Lan DM, Liu FT, Zhao J, Chen Y, Wu JJ, Ding ZT, et al. Effect of trehalose on PC12 cells overexpressing wild-type or A53T mutant alpha-synuclein. Neurochem Res 2012;37(9):2025–32.
[14] He Q, Koprich JB, Wang Y, Yu WB, Xiao BG, Brotchie JM, et al. Treatment with trehalose prevents behavioral and neurochemical deficits produced in an AAV alpha-synuclein rat model of Parkinson's disease. Mol Neurobiol 2015.
[15] Aguib Y, Heiseke A, Gilch S, Riemer C, Baier M, Schatzl HM, et al. Autophagy induction by trehalose counteracts cellular prion infection. Autophagy 2009;5(3):361–9.
[16] Beranger F, Crozet C, Goldsborough A, Lehmann S. Trehalose impairs aggregation of PrPSc molecules and protects prion-infected cells against oxidative damage. Biochem Biophys Res Commun 2008;374(1):44–8.
[17] Wang X, Fan H, Ying Z, Li B, Wang H, Wang G. Degradation of TDP-43 and its pathogenic form by autophagy and the ubiquitin-proteasome system. Neurosci Lett 2010;469(1):112–6.
[18] Honda Y, Tanaka M, Honda S. Trehalose extends longevity in the nematode Caenorhabditis elegans. Aging Cell 2010;9(4):558–69.
[19] Minutoli L, Altavilla D, Bitto A, Polito F, Bellocco E, Lagana G, et al. The disaccharide trehalose inhibits proinflammatory phenotype activation in macrophages and prevents mortality in experimental septic shock. Shock 2007;27(1):91–6.
[20] LaRocca TJ, Henson GD, Thorburn A, Sindler AL, Pierce GL, Seals DR. Translational evidence that impaired autophagy contributes to arterial ageing. J Physiol 2012;590(Pt 14):3305–16.
[21] Echigo R, Shimohata N, Karatsu K, Yano F, Kayasuga-Kariya Y, Fujisawa A, et al. Trehalose treatment suppresses inflammation, oxidative stress, and vasospasm induced by experimental subarachnoid hemorrhage. J Transl Med 2012;10:80.
[22] Lotfi P, Tse DY, Di Ronza A, Seymour ML, Martano G, Cooper JD, et al. Trehalose reduces retinal degeneration, neuroinflammation and storage burden caused by a lysosomal hydrolase deficiency. Autophagy 2018;14:1419–14348.
[23] Sarkar S, Rubinsztein DC. Small molecule enhancers of autophagy for neurodegenerative diseases. Mol Biosyst 2009;4:895–901.
[24] Mardones P, Rubinsztein DC, Hetz C. Mystery solved: trehalose kickstarts autophagy by blocking glucose transport. Sciencesignaling 2016;9:416fs2.
[25] Felice VD, Quigley EM, Sullivan AM, O'Keeffe GW, O'Mahony SM. Microbiota-gut-brain signalling in Parkinson's disease: Implications for non-motor symptoms. Parkinsonism Relat Disord 2016;27:1–8.
[26] Ruf J, Wacker H, James P, Maffia M, Seiler P, Galand G, et al. Rabbit small intestinal trehalase. Purification, cDNA cloning, expression, and verification of glycosylphosphatidylinositol anchoring. J Biol Chem 1990;265(25):15034–9.
[27] Nwaka S, Holzer H. Molecular biology of trehalose and the trehalases in the yeast Saccharomyces cerevisiae. Prog Nucleic Acid Res Mol Biol 1989;58:197–237.

[28] Ishihara R, Taketani S, Sasai-Takedatsu M, Kino M, Tokunaga R, Kobayashi Y. Molecular cloning, sequencing and expression of cDNA encoding human trehalase. Gene 1997;202(1–2):69–74.
[29] Oesterreicher TJ, Markesich DC, Henning SJ. Cloning, characterization and mapping of the mouse trehalase (Treh) gene. Gene 2001;270(1–2):211–20.
[30] Oesterreicher TJ, Nanthakumar NN, Winston JH, Henning SJ. Rat trehalase: cDNA cloning and mRNA expression in adult rat tissues and during intestinal ontogeny. Am J Physiol 1998;274(5 Pt 2):R1220–7.
[31] Sacktor B. Trehalase and the transport of glucose in the mammalian kidney and intestine. Proc Natl Acad Sci U S A 1986;60(3):1007–14.
[32] Bergoz R. Trehalose malabsorption causing intolerance to mushrooms. Report of a probable case. Gastroenterology 1971;60(5):909–12.
[33] Sasai-Takedatsu M, Taketani S, Nagata N, Furukawa T, Tokunaga R, Kojima T, et al. Human trehalase: characterization, localization, and its increase in urine by renal proximal tubular damage. Nephron 1996;73(2):179–85.
[34] van Handel E. Do trehalose and trehalase function in renal glucose transport? Science 1969;163(3871):1075–6.
[35] van Handel E. Trehalase and maltase in the serum of vertebrates. Comp Biochem Physiol 1968;26(2):561–6.
[36] Eze LC, Evans DA. Plasma trehalase activity in diabetes mellitus. Clin Chim Acta 1970;28(1):153–9.
[37] Baumann FC, Boizard-Callais F, Labat-Robert J. Trehalase activity in genetically diabetic mice (serum, kidney, and liver). J Med Genet 1981;18(6):418–23.
[38] Buts JP, Stilmant C, Bernasconi P, Neirinck C, De Keyser N. Characterization of alpha-trehalase released in the intestinal lumen by the probiotic Saccharomyces boulardii. Scand J Gastroenterol 2008;43(12):1489–96.
[39] Welsh JD, Poley JR, Bhatia M, Stevenson DE. Intestinal disaccharidase activities in relation to age, race, and mucosal damage. Gastroenterology 1978;75(5):847–55.
[40] Gudmand-Høyer E, Fenger HJ, Skovbjerg H, Kern-Hansen P, Madsen PR. Trehalase deficiency in Greenland. Scand J Gastroenterol 1988;23(7):775–8.
[41] Yoshida K, Mizukawa H, Haruki E. Serum trehalase activity in patients with rheumatoid arthritis. Clin Chim Acta 1993;215(1):123–4.
[42] Eze LC. Plasma trehalase activity and diabetes mellitus. Biochem Genet 1989;27(9–10):487–95.
[43] Galand G. Brush border membrane sucrase-isomaltase, maltase-glucoamylase and trehalase in mammals. Comparative development, effects of glucocorticoids, molecular mechanisms, and phylogenetic implications. Comp Biochem Physiol. B 1989;94(1):1–11.
[44] Martano G, Gerosa L, Prada I, Garrone G, Krogh V, Verderio C, et al. Biosynthesis of astrocytic trehalose regulates neuronal arborization in hippocampal neurons. ACS Chem Neurosci. 2017;8(9):1865–72.
[45] Mayer AL, Higgins CB, Heitmeier MR, Kraft TE, Qian X, Crowley JR, et al. SLC2A8 (GLUT8) is a mammalian trehalose transporter required for trehalose-induced autophagy. Sci Rep 2016;6:38586.
[46] Chen X, Quan Y, Wang H, Luo H. Trehalase regulates neuroepithelial stem cell maintenance and differentiation in the Drosophila optic lobe. PLoS One 2014;9(7):e101433.
[47] Ouyang Y, Xu Q, Mitsui K, Motizuki M, Xu Z. Human trehalase is a stress responsive protein in Saccharomyces cerevisiae. Biochem Biophys Res Commun 2009;379(2):621–5.